BBA - Molecular Cell Research 1869 (2022) 119343

Contents lists available at ScienceDirect

BBA - Molecular Cell Research

journal homepage: www.elsevier.com/locate/bbamcr

Research Paper

Mechanism of apoptosis activation by Curcumin rescued mutant p53Y220C in human pancreatic cancer

Lakshay Malhotra [a], Saurabh Sharma [a], Gururao Hariprasad [a], Renu Dhingra [b], Vandana Mishra [c], Radhey S. Sharma [c], Punit Kaur [a], Abdul S. Ethayathulla [a,*]

[a] Department of Biophysics, All India Institute of Medical Sciences, New Delhi 110029, India
[b] Department of Anatomy, All India Institute of Medical Sciences, New Delhi 110029, India
[c] Bioresources and Environmental Biotechnology Laboratory, Department of Environmental Studies, University of Delhi, Delhi 110007, India

ARTICLE INFO

Keywords:
Apoptosis
Bio-layer interferometry
Post-translational modification (PTM)
Circular dichroism (CD)
Flow cytometry
Immunoblotting
Immunocytochemistry
Label free proteomics
Pancreatic cancer
Protein purification
p53
Protein drug interaction

ABSTRACT

The mutant p53Y220C (mutp53Y220C) is frequently observed in numerous tumors, including pancreatic cancer. The mutation creates a crevice in the DNA binding core domain and makes p53 a thermally unstable non-functional protein that assists tumor progression and confers resistance to chemotherapeutic drugs. Restoring mutp53 function to its wild type by selectively targeting this crevice with small molecules is a pivotal strategy to promote apoptosis. In this study, we have shown through different biophysical and cell-based studies that curcumin binds and rescues mutp53Y220C to an active wild-type conformation and restores its apoptotic transcription function in BxPC-3-pancreatic cancer cells. In addition, the curcumin-rescued-p53Y220C (CRp53) showed significant hyperphosphorylation at Ser15, Ser20, and acetylation at Lys382 with an 8-fold increase in transcription activity in the BxPC-3 cell lines. We also observed that the active CRp53 escapes Mdm2-mediated proteasomal degradation and the majority of the proteins were localized inside the nucleus with an increased half-life and transcription restoration compared to untreated BxPC-3 cells. By label-free proteomics analysis, we observed that upon curcumin treatment almost 227 proteins were dysregulated with the majority of them being transcriptional targets of p53. Based on our studies, it reflects that apoptosis in pancreatic cancer cells is mediated by curcumin-rescued mutant p53Y220C.

1. Introduction

The p53 tumor suppressor protein is the master regulator of downstream effector genes involved in cell cycle arrest, senescence, and apoptosis to prevent cell proliferation and cancer development [1–3]. Specific kinases like ATM/ATR, Chk1, Chk2, CK, HIPK2, *etc,*. activate p53 to perform the tumor suppressor activity in cancer cells [2,4]. To date, ten different phosphorylation sites Ser15, Ser20, Ser33, Ser46, Ser366, Ser392, Thr18, Thr304, Thr377, and Thr387 have been detected in different cancer lines to induce p53-mediated apoptosis [2,5]. More importantly, many cancer therapies rely on p53-mediated apoptosis to suppress tumor development after the generation of cellular stimulus induced by drugs [6,7]. Furthermore, the efficacy of widely used chemotherapeutic drug-like 5-fluorouracil also partly depends on the p53-mediated apoptosis and cell growth arrest in various cancers like breast cancer, pancreatic cancer, colorectal cancer, and other solid tumors [8–10]. But in the majority of human cancers, alteration in p53 by a missense mutation in the DNA-binding domain (DBD) results in loss of its ability to bind target gene promoter site and exhibit tumor suppressor activity. Moreover, loss of transcription activity leads to invasion, metastasis, and poor prognosis in many cancers like pancreatic cancer [11,12], astrocytoma [13], lung cancer [14], and breast cancer [15,16]. In some cases, missense mutations in p53 make cancer cells resistant to chemo drugs leading to relapse of the tumor [17–19]. Current clinical strategies are to reintroduce p53 in tumors [20–22] or to restore the mutant p53 transcription function by molecular chaperones or small molecule drugs to activate downstream anticancer signalling pathway genes [23–25]. The p53Y220C is one of the high frequent p53 mutants found in >100,000 cancer cases reported every year [26–28]. The mutation of Tyr to Cys in the DNA binding domain leads to the formation of

Abbreviations: BLI, Bio-layer interferometry; CD, Circular dichroism; CK, Casein kinase; CRp53, Curcumin-rescued p53Y220C; PTM, Post translational modification; p53Y220C FL, p53Y220C full length; wt, wild-type.

* Corresponding author.
E-mail address: ethayathulla@aiims.edu (A.S. Ethayathulla).

https://doi.org/10.1016/j.bbamcr.2022.119343
Received 4 April 2022; Received in revised form 17 August 2022; Accepted 17 August 2022
Available online 22 August 2022

a shallow cavity between S3/S4 and S7/S8 loops with a global change in the overall stability of the protein. The p53Y220C is known as a temperature-sensitive mutant as it destabilizes at physiological conditions to form aggregates [29]. The thermal stability of the protein is decreased by 4.2 kcal/mol resulting in the loss of its ability to bind promoter and perform tumor suppressor activity [30]. The mutation-induced crevice is far from the DNA recognizing region of the protein making it an ideal druggable cavity to design small chaperone molecules to increase its thermal stability and rescue its transcription function. Hence, the hunt for effective ligands to restore p53Y220C mutant function is very much alive. Many synthetic compounds such as sulfonylpyrimidines, phikan083, MB725, PK5174, PK5196, PK7088, and natural ligands like ashwagandha derived withanolides were also reported to bind and stabilize the p53Y220C mutant [31–38]. However, some of these drugs are coupled with several adverse effects like higher cellular toxicity or the inability to completely activate mutant p53 to function-like wild type [39,40]. In this study, we show that curcumin could stabilize mutant p53Y220C and restore its transcription function to initiate downstream intrinsic and extrinsic apoptotic signalling pathways in BxPC-3 cell lines using label-free proteomics and cell-line-based assays. This is the first report of post-translational modifications analysis of mutant p53Y220C before and after drug treatment to establish that the curcumin-rescued p53Y220C (CRp53) is functionally active. We also propose a possible mechanism by which CRp53 activates apoptotic pathways in the human pancreatic cancer cell line. We thus provide the first line of evidence that curcumin can be used as combinatorial therapy for the treatment of cancers harboring p53Y220C mutation.

2. Materials and methods

2.1. Antibodies from cell signalling technology

Cleaved caspase-3 rabbit mAb (9664), caspase-3 rabbit mAb (14220), PARP antibody (9542) rabbit mAb, cleaved PARP rabbit mAb (5625), caspase-7 (12827) rabbit mAb, cleaved caspase-7 (8438) rabbit mAb, p53 (7f5) (2527) rabbit mAb, P-p53 Ser20 (9287) rabbit mAb, P-p53 Ser392 (9281) rabbit mAb, P-p53 Ser46 (2521) rabbit mAb, P-p53 Ser15 (9284) rabbit mAb, P-p53 Ser9 (9288) rabbit mAb, acetyl-p53 Lys379/382 (2525) rabbit mAb, P-p53 Ser33 (2526) rabbit mAb, anti-IgG HRP linked antibody (7074).

2.2. Other antibodies

Bax, Abkine (ABP55948) rabbit mAb, Bcl-2, Abkine (ABP56021) rabbit mAb, ATR rabbit mAb (Abclonal A7247), Chk1 rabbit mAb (Abclonal A4194), ATM mAb (Abclonal AP19650), Chk2 rabbit mAb (Abclonal A19543), P-Chk2 Ser6 rabbit mAb (Abclonal AP0676); human Mdm2 rabbit pAb (Abclonal A13327); GAPDH rabbit mAb (Abclonal A19056).

2.3. CD spectroscopy

The Far-UV spectra (200-250 nm) of full-length p53Y220C and wild-type p53 were monitored using a JASCO J-1500 CD spectrophotometer using a quartz cuvette of 0.1 cm path length. The CD spectra were taken in duplicates both in the presence and absence of curcumin for p53Y220C FL. A ratio of 1:1 was used to measure the spectra of p53Y220C FL with curcumin (Sigma Aldrich PCode: 1002542749) [36]. An average of two CD spectra were used to plot the graph using SigmaPlot 14.0 (n = 2).

2.4. Bio-layer interferometry (BLI)

The BLI experiment was performed using the OCTET RED R8 system (Sartorius). At first, the biotinylated p53 antibody (DO7) was immobilized/loaded on SAX (high precision streptavidin sensor) for 600 s at 700 rpm. The antibody-loaded sensor was then washed with PBS for the 60 s and then baselined in assay buffer for 60 s at 700 rpm. Then, the BxPC-3 cell lysate was used for enriching the p53Y220C on the p53 antibody-bound sensor for 8 h at 15 °C at 700 rpm followed by washing in PBS of pH 7.5, 5.5, and 3.5, respectively, for removing the nonspecific proteins for 60 s, 180 s and 180 s, respectively, at 700 rpm. The enrichment was also conducted on a reference sensor without any antibody. After the p53 enrichment, the same sensors were used for curcumin binding affinity estimation by using different curcumin concentrations in PBS pH 7.5, (0, 0.195, 0.39, 0.78, 1.56, 3.125, 6.25, 12.5, 25, 50 μM). For this kinetic experiment for each concentration, first, the baseline of 60 s was taken in the PBS followed by the association set up for 200 s for the different curcumin concentrations followed by the dissociation in the PBS for the same time interval with 1000 rpm [40–43]. The experiment was performed thrice, and the results were analyzed using BLI analysis studio 12.2.0.20, and K_d was calculated after subtracting the reference values, followed by aligning data to the average baseline step on Y-axis, and aligning inter-step correlation to the baseline step and using the Savitsky-Golay Filtering (n = 3). The same experiment was done on the Bewo cell line lysate having p53 wt, as the control using the Sartorius Octet R8.

2.5. Cell culture

The BxPC-3 (human p53Y220C pancreatic cell line) cells were purchased from ATCC (Manassas, VA, USA). Cells were frozen at −174 °C in LN2 container in multiple vials and cultured for <15 doubling the population for the present study. RPMI-1640 Media (Gibco, Thermo Fisher Scientific) with 10 % fetal bovine serum (South American Origin, Gibco) and 1 % antibiotic-antimycotic (100×) (Gibco) were used for culturing. Cells were stored at 37 °C and maintained in Thermoscientific humified incubator with 5 % CO_2 (LEGENDRE, SOOKDEO, and FOSTER 2014). 1× Trypsin 0.25 % and 0.2 % EDTA (in Dulbecco's phosphate-buffered saline (Himedia)) were used for cell dissociation during cell passaging.

2.6. Cell cytotoxicity assay

The cytotoxicity of natural compound curcumin in BxPC-3 p53Y220C genomic mutant cell lines was measured using an MTT assay at different time intervals (6, 8, 10, 12, 14, 16, 24, 48, 72 h) with the same protocol as described in our previous study [36]. All the data were represented as median ± standard error of the mean (n = 4).

2.7. Luciferase reporter assay

The pGL-3 plasmids containing full-length Mdm2 and p21 promoters purchased from AddGene, MA USA were transfected into the BxPC-3 cells using the Lipofectamine 2000 (Invitrogen, Carlsbad CA, USA). After 32 h of transfection, the cells were treated with 3 and 8 μM of curcumin for 16 h, and then the Luciferase activity was detected using the Dual-Luciferase® Reporter Assay System (Promega, WI, USA) following the manufacturer's protocol. For the assay, the transfection control (No vector), and curcumin control were also used. And the graph was plotted in GraphPad Prism 8 using the relative fold change (luminescence intensity of the test for the transfection control). All the data were represented as median ± standard error of the mean (n = 2).

2.8. ELISA

The BxPC-3 cells were treated with 3, and 8 μM of curcumin for 24 h and then lysed with RIPA lysis buffer along with 1× protease inhibitor cocktail on ice and then centrifuged at 13,000 rpm for 15 min at 4 °C. Total protein of 30 μg quantified using Bradford reagent was used for ELISA. The p21 and Mdm2 ELISA kits (Real gene) were used following

the manufacturer's protocol. The ELISA was performed four times and the graph was plotted using GraphPad Prism 8. All the data were represented as median ± standard error of the mean (n = 4).

2.9. Caspase-3 activity assay

The caspase-3 activity was estimated for BxPC-3 cell lysates in the presence and absence of 3 and 8 μM curcumin (24 h incubation). The experiment was performed in 3 replicates using the same protocol described in our previous studies [36]. All the data were represented as median ± standard error of the mean (n = 3).

2.10. Immunofluorescence

The immunofluorescence studies were conducted for BxPC-3 cells in the presence and absence of 3 and 8 μM curcumin after 24 h treatment. The immunofluorescence was performed using the same protocol as reported in our previous study [36]. The images were taken at 20× magnification using the Nikon DS-Qi2. The total number of cells with enhanced nuclear signal was counted along with the total number of cells.

2.11. Annexin V and PI by flow cytometry

The apoptotic population of the BxPC-3 cells after 8 μM of curcumin treatment for 24 h was measured using the Alexa fluor 488 conjugated Annexin V and PI apoptosis assay kit (Invitrogen) following manufacturer protocol. The data was acquired by BD LSR II (USA) and analyzed using Flowjo-10 (TreeStar, USA) software (n = 3).

2.12. Cytotoxicity in the presence of Pifithrin α

The MTT assay was performed using the above same protocol at 3, 8 and 10 μM curcumin concentrations along with different Pifithrin α (Sigma Aldrich) concentrations (10,15 and 20 μM) [44,45]. The experiment was conducted in 8 replicates. The data was analyzed using Sigmaplot 10 and all the data were represented as median ± standard error of the mean (n = 8).

2.13. Cytotoxicity in the presence of Nutlin-3a

The MTT assay was performed using the above same protocol at 3, 8 and 10 μM curcumin concentrations along with different Nutlin-3a (Sigma Aldrich) concentrations (5, 10 and 15 μM) [35,44]. The experiment was conducted in 8 replicates. The data was analyzed using Sigmaplot 10 and all the data were represented as median ± standard error of the mean (n = 8).

2.14. Immunoblotting

The BxPC-3 cells were cultured and treated with 3 and 8 μM of curcumin for 24 h and then further lysed using the RIPA lysis buffer, containing both 1× phosphatase and protease inhibitor cocktail (Promega and Abcam). The lysate was centrifuged for 15 min at 13,000 rpm at 4 °C. The protein supernatant was then quantified using the Bradford assay (Biorad). A 30 μg of the cell lysate resolved using 12 % SDS-PAGE was transferred to methanol charged PVDF (polyvinylidene difluoride) membrane (Biorad). The membrane was initially blocked with 5 % BSA overnight, followed by incubation with primary antibody for 12 h at 4 °C. After three TBST washes for 5 min, the blot was incubated with HRP conjugated anti-rabbit IgG for 2 h. The blots were then washed with TBST thrice, followed by the development with the ECL (enhanced chemiluminescence reaction). The blots were then visualized on the Azure C-400 gel documentation system using the FITC fluorescence filter. All the blots were repeated twice (n = 2). The image densitometry quantification was performed using ImageJ software and the densitometry plots were made using Sigmaplot 10.

2.15. Sample preparation for whole-cell proteomics

2×10^6 BxPC-3 cells were seeded in T-75 flasks in 15 mL of complete RPMI-1640 media and incubated with 5 % CO_2 till the confluency reached 60–70 %, followed by treatment of 3 and 8 μM of curcumin for 24 h. Then the cells were harvested using 0.25 % Trypsin and 0.2 % EDTA. The cells were pelleted and stored at −80 °C.

2.16. Two-dimensional gel electrophoresis and analysis of gel images

A 2-dimensional (2D) gel electrophoresis was performed for 3 and 8 μM curcumin-treated BxPC-3 cells for 24 h. A total protein of 80 μg was mixed with the rehydration buffer containing 7 M urea, 2 M thiourea, 2 % CHAPS with 0.2 % ampholyte, and 40 mM DTT (dithiothreitol). The IEF (isoelectric focusing) was performed by Protein IEF Cell (Bio-Rad, Hercules, CA, USA) using the manufacturer's protocol. The samples were initially separated in the 1st-dimension using 7 cm immobilized pH gradient (IPG) strips of pH 4–7 (Bio-Rad, Hercules, CA, USA). The cycle used for IEF was 200 V for 1 h followed by 500 V for 1 h, the next 1 h for 1000 V and the final treatment for 5 h at 8000 V with a total of 13,000 VH. The IPG strips were equilibrated with a buffer containing 50 mM Tris-HCl (pH - 8.8), 6 M urea, 4 % (w/v) SDS, 20 % (w/v) glycerol, 10 mg/mL DTT and 40 mg/mL iodoacetamide (Sigma-Aldrich, St. Louis, MO, USA) for 20 min. The protein samples were then subjected to a 2nd dimension using the SDS-PAGE (15 and 5 % gel system). The gels were then silver stained and captured using the Azure C-400 Gel documentation system (n = 3).

2.17. Sample preparation for LFQ (label-free quantification)

The cell pellets were washed thrice with 1× TBS (Tris saline) followed by the addition of the protease inhibitor (Roche). The pellets were resuspended and vortexed after the addition of hot boiling GN buffer (6 M guanidium HCl and 0.1 M Tris pH 8.5), followed by the incubation of 5 min at 100 °C. The samples were then kept in ice and subjected to sonication for 3 min (1 s pulse and 1 s rest) for the breakdown of nucleic acids and solubilization of the membrane proteins. The samples were further centrifuged at 10,000 rpm for 5 min for the complete lysis. The clear supernatant was taken in a fresh tube and the protein was quantified using the Bradford to take an equal amount from each sample for the in-digestion protocol. 25 μL of BxPC-3 cell lysate were taken and then reduced with 5 mM TCEP and further subjected to alkylation with 50 mM iodoacetamide followed by Trypsin digestion (1:50, Trypsin/lysate ratio) for 16 h at 37 °C. The salt from the BxPC-3 whole cell lysate digests was removed using the C18 silica cartridge and then the digests were dried using the speed vac. The dried pellet was resuspended in buffer A (5 % acetonitrile, 0.1 % formic acid).

2.18. Mass spectrometric analysis of peptide mixtures

All the experiments were performed using EASY-nLC 1000 system (Thermo Fisher Scientific) coupled to Thermo Fisher-QExactive equipped with a nanoelectrospray ion source. The peptide mixture of 1 μg concentration was resolved using a 15 cm PicoFrit column (360 μm outer diameter, 75 μm inner diameter, 10 μm tip) filled with 2 μm of C18-resin (Dr. Maeisch, Germany). The peptides were loaded with buffer A and then eluted with a 0–40 % gradient of buffer B (95 % acetonitrile, 0.1 % formic acid) at a flow rate of 300 nL/min for 100 min. MS data were acquired using a data-dependent top 10 method dynamically choosing the most abundant precursor ions from the survey scan.

2.19. Data processing

All samples were processed, and RAW files generated were analyzed

with Proteome Discoverer (v2.2) against the Uniprot HUMAN reference proteome database. For the Sequest search, the precursor and fragment mass tolerances were set at 10 ppm and 0.5 Da, respectively. The protease used to generate peptides, *i.e.*, enzyme specificity was set for Trypsin/P (cleavage at the C terminus of "K/R": unless followed by "P") along with a maximum missed cleavages value of two. Carbamidomethyl on cysteine as fixed modification and oxidation of methionine and N-terminal acetylation were considered as variable modifications for database search. Both peptide spectrum match and protein false discovery rate were set to 0.01 FDR. The protein FDR confidence combined was set to be high, and only master proteins were selected. Also, the unique peptide was set to $\geq$2, followed by the selection of only those proteins with false contamination status. As the experiment was done in 4 replicates, the proteins whose abundance was high in at least 3 replicates were selected and then analyzed using Panther pathways as well as Cytoscape using the .tsv files of the string database of 0.700 confidence values, followed by the fetching of the FI annotations and categorizing the proteins based on their different pathways. The dysregulated proteins were searched as p53 targets using the hTFtarget server [46]. The mass spectrometry proteomics data have been deposited to the ProteomeXchange Consortium through the PRIDE [47] partner repository with the dataset identifier "PXD030802".

2.20. Statistics

One-way ANOVA is used for luciferase reporter assay, caspase-3 activity assay, ELISA experiments, Pifithrin α and Nutlin-3a experiments and the SD is calculated wherever applicable.

2.21. Data availability

The mass spectrometry proteomics data have been deposited to the ProteomeXchange Consortium through the PRIDE partner repository with the dataset identifier "PXD030802". The other experimental data sets are available from the corresponding author on reasonable request.

3. Results

3.1. Restoration of full length mutant p53Y220C conformation by curcumin

The CD spectra of full-length mutant p53Y220C showed that the

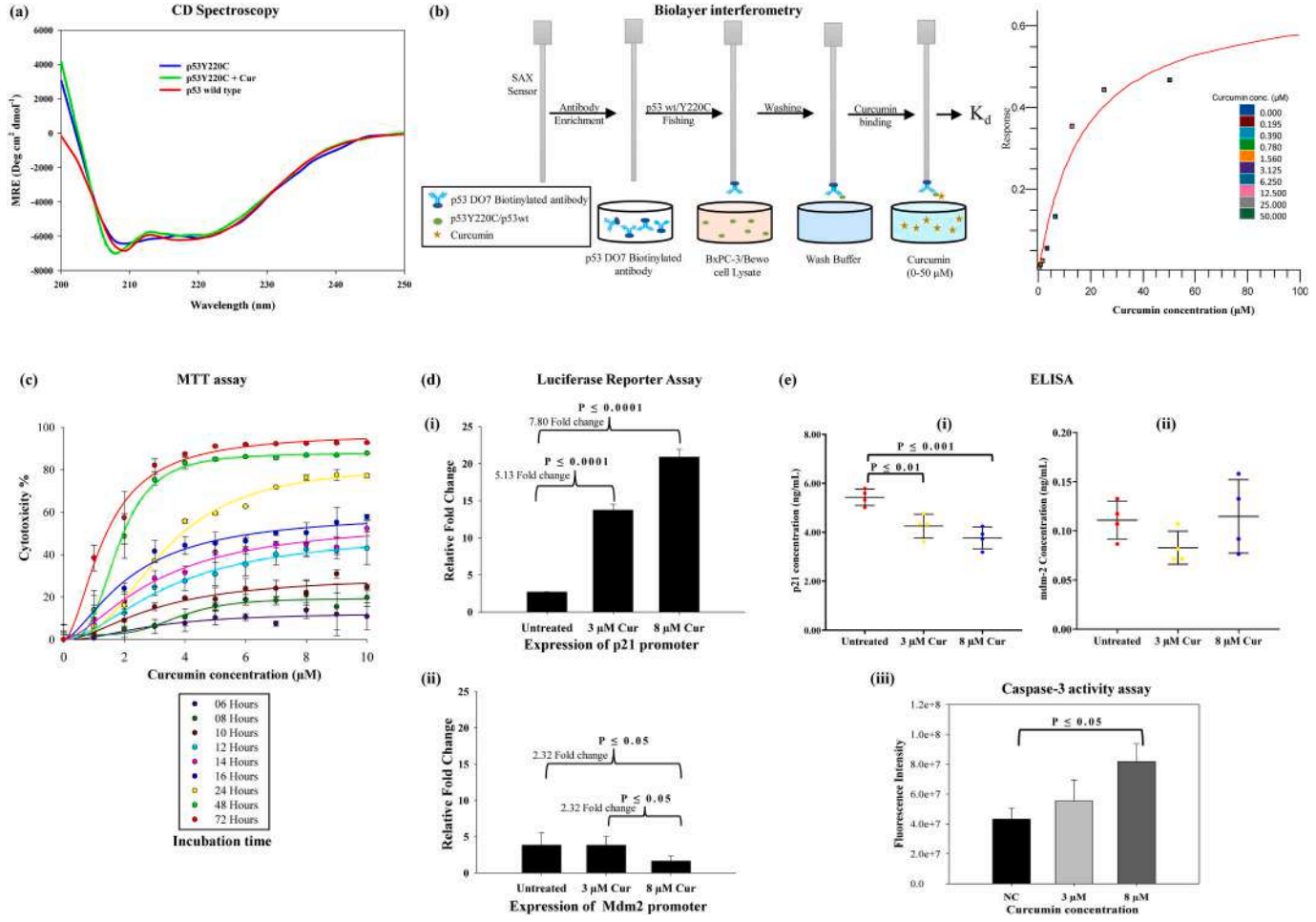

Fig. 1. *In vitro* and *in vivo* curcumin binding with p53 wt and mutant p53Y220C. (a) The Far-UV CD spectra of p53 wt (red), p53Y220C in the absence (blue) and presence (green) of curcumin in 1:1 ratio (n = 2). (b) Bio-layer interferometry analysis of curcumin binding with p53 wt and p53Y220C: The figure represents experimental visualization of the workflow used in the BLI. The p53 Biotinylated antibody was enriched using SAX biosensor and proteins p53 wt/p53Y220C were enriched from the Bewo/BxPC-3 cell lysate respectively. The binding affinity of curcumin with p53Y220C from BxPC-3 cells was found to be 17 ± 5 µM (n = 3). (c) Cytotoxicity of curcumin on BxPC-3 cell lines was measured at different concentrations (0–10 µM) and different time intervals (6 to 72 h) (n = 4). (d) Luciferase reporter assay to measure transcription activity of p53Y220C in the absence and presence of 3 and 8 µM curcumin using (i) p21 and (ii) Mdm2 promoter (n = 2) (P ≤ 0.0001, P ≤ 0.05). (e) Represents the protein concentration of (i) p21 and (ii) Mdm2 measured using ELISA before and after 3 and 8 µM curcumin treatment in the BxPC-3 cell line (n = 4) (P ≤ 0.01; P ≤ 0.001). (iii) Caspase-3 activity assay before and after 3 and 8 µM curcumin treatment in the BxPC-3 cell line (n = 3) (P ≤ 0.05). (For interpretation of the references to color in this figure legend, the reader is referred to the web version of this article.)

protein has less ordered α-helices compared to the wild type (Fig. 1a). An increase in negative ellipticity at 208 nm was observed upon the addition of curcumin (ratio 1:1) due to π to π* transitions indicating the stability of the protein like wild-type (Fig. 1a). The study indicates that the curcumin restores the secondary structure of p53Y220C.

3.2. Curcumin binds to cellular mutant p53Y220C

The kinetic measurements using label-free optical biosensors showed that the curcumin binds to mutant p53Y220C with dissociation constant $K_d = 17 \pm 5$ μM ($Chi^2 = 0.0133$ and $R^2 = 0.9597$) (Figs. 1b, S1a). Surprisingly, no binding was observed for p53 wt (Bewo placental cell line), and the experiments were repeated thrice (Fig. S1a). The study shows that curcumin binds to the crevice in mutant protein due to the substitution of Tyr to Cys which is absent in wild type.

3.3. Curcumin induces cell death in BxPC-3 pancreatic cancer cells

Curcumin-induced cytotoxicity in BxPC-3 p53Y220C mutant cell lines showed that until 6 h, only 10 % cell death was observed at 10 μM curcumin concentration and by 16 h, the IC_{50} was in the range of 8 μM. However, with 5 μM curcumin concentration ~90 % cytotoxicity could be observed after 72 h drug treatment (Fig. 1c). Interestingly, in the p53 null cell line Saos-2 (control), even at 10 μM of curcumin treatment only 14 % cytotoxicity was observed after 72 h (Fig. S1b). Hence, we have selected 3 μM [36] and 8 μM of curcumin concentrations (24 h) for further experiments.

3.4. Curcumin restores the transcriptional activity of mutp53Y220C

The transcriptional activity of curcumin-rescued p53Y220C (CRp53) measured with p21 promoter in BxPC-3 cell lines showed a 5-to-8-fold relative increase in p21 expression ($P \leq 0.0001$) at 3 and 8 μM of curcumin concentration (Fig. 1d(i)) [45–47]. Although an 8-fold increase in p21 promoter activity was observed, the ELISA showed a decrease in p21 protein concentration (Fig. 1e(i)). The decrease in p21 might be due to the degradation or inactivation of p21 by caspase-3 mediated decay shown by an increase in the caspase-3 activity after curcumin treatment (Fig. 1e(iii)). The caspase-3 (DEVD Caspase) is known to cleave and inactivate the cyclin-dependent kinase inhibitor p21/Waf1/Cip1, which is a negative regulator of p53-dependent apoptosis [48–50]. Inactivation of p21 or repression of p21 may mediate p53-dependent apoptosis in BxPC-3 cell lines [51,52]. While in the case of Mdm2 surprisingly, a 2-fold relative decrease in Mdm2 expression was observed upon 8 μM ($P \leq 0.05$) curcumin treatment (Fig. 1d(ii)). The ELISA also showed no change in expression of Mdm2 (Fig. 1e(ii)) indicating that CRp53 has more specificity toward activating caspase-3 mediated apoptosis in BxPC-3 pancreatic adenocarcinoma cell lines.

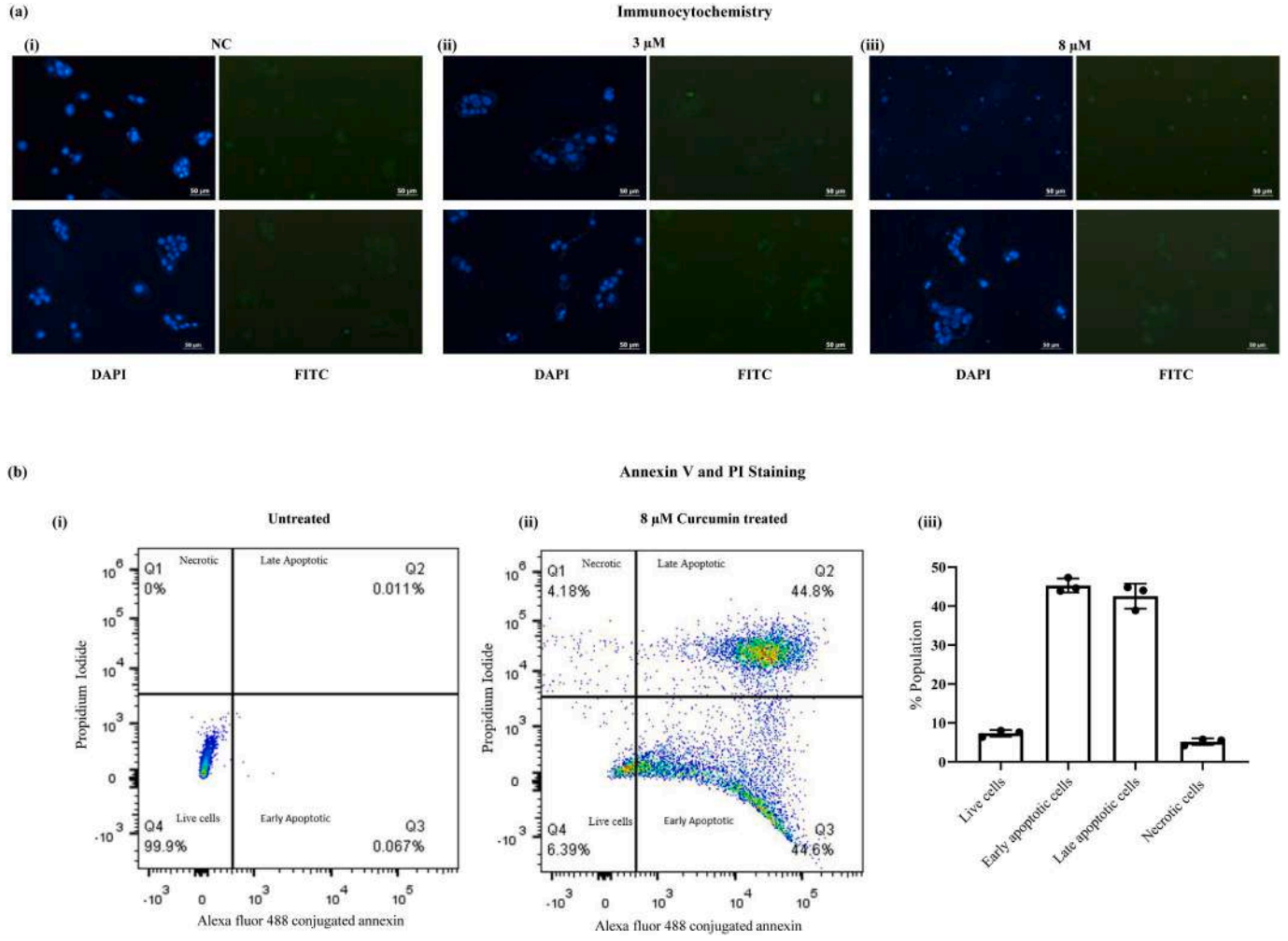

Fig. 2. Distribution of p53Y220C before and after curcumin treatment in BxPC-3 cell lines. (a) FITC and DAPI images of (i) negative control untreated BxPC-3 cells (ii) cells treated with 3 μM and (iii) 8 μM curcumin for 24 h. (b) Annexin V and PI assay of BxPC-3 cell lines using flow cytometry. The distribution of cells at different phases (i) before and (ii) after 24 h 8 μM curcumin treatment (n = 3). (iii) Graphical distribution of the different populations of cells treated with 8 μM curcumin for 24 h (n = 3).

3.5. Nuclear export of CRp53 and apoptosis in BxPC-3 cells

To understand the distribution of CRp53 in pancreatic adenocarcinoma cells, immunocytochemistry was performed. In the untreated BxPC-3 cells, the mutant p53Y220C was found to be distributed throughout the cell (Fig. 2a(i)). However, in 3 μM and 8 μM curcumin treatment, around 54 % and 82.5 % of cells showed the mutant p53Y220C protein is more localized inside the nucleus, respectively (Fig. 2a(ii) and (iii)) (Table S1). The cell projections showed less extentions compared to the untreated cells, suggesting the occurrence of apoptosis in the cell line (Fig. 2a). In 8 μM of curcumin-treated cells, a drastic change in the cell morphology was observed indicating apoptosis (Fig. 2a(iii)) (Table S1). To estimate the number of cells in early and late apoptosis after 8 μM curcumin treatment, flow cytometry analysis was performed (Fig. 2b). Based on the 10,000 events, 45.26 ± 1.8 % of the population of cells were in early apoptosis, 42.57 ± 3.20 % in late apoptotic phase, 4.82 ± 0.84 % in the necrotic phase, and approximately 7.34 ± 0.85 % cells were alive (Fig. 2b(ii)). The flow cytometry clearly shows that curcumin induces almost 87.83 ± 2.76 % of cells to the apoptotic phase (Fig. 2b(iii)). Hence, increased CRp53 distribution inside the nucleus and more cells in the apoptotic phase (Fig. 2a) indicates the nuclear transport of functionally restored mutant p53 inside the nucleus.

3.6. Post-translational modifications in CRp53 for apoptotic activity

The post-translational modifications (PTM) of mutant p53 in BxPC-3 cell lines showed a basal level of phosphorylation at Ser9, Ser33, Ser46, Ser392 and acetylation at Lys382. The mutant protein with basal level PTM is in the functionally inactive or "pseudo" wild-type like conformation (Figs. 3a–b, S2). While in the CRp53, significant hyperphosphorylation was observed at Ser15, Ser20, and acetylation at Lys382 (Figs. 3a, S2). Interestingly, a dimeric form (Ser9, Ser15, and Ser20) and the truncated form (Ser20, Ser33, and Lys382) of CRp53 (Figs. 3a–b, S2) were also observed in the curcumin-treated cells. All these PTMs indicate that the CRp53 is recognized by PI3 kinases like ATM/Chk2/HIPK2 to activate p53 and initiate apoptosis in BxPC-3 cells [51,53,54]. To identify the PI3 kinases responsible for PTMs in CRp53, the expression of various kinases was analyzed before and after curcumin treatment (Figs. 3c, S3). The expression of kinases ATM, ATR, Chk-1, Chk-2 and HIPK2 was found to be elevated indicating their active state to perform PTMs in p53 [5,53,55–58]. The kinase ATM and ATR phosphorylate CRp53 at Ser15 [59] and HIPK2 at Ser46 [60]. While different phosphorylated active forms of Chk-2 (data not shown) and Chk-1 kinases activate CRp53 at Ser15 and Ser20 [54,61,62]. Interestingly, Phospho-Chk-2 Ser516 expression was found to be significantly elevated compared to untreated cells (Figs. 3c–d, S3). The P-Chk-2 Ser516 is known to activate p53 wt upon apoptotic stimuli in normal cells [63–67]. Hence, the PTM analysis shows that the curcumin-rescued mutant p53Y220C gets activated by the PI3 kinases to perform apoptosis in BxPC-3 cells.

3.7. CRp53 induced apoptosis in pancreatic adenocarcinoma cells

To establish that the apoptosis induced in BxPC-3 cells is mediated by the transcription activity of the curcumin-rescued mutant p53, the cells were treated with Pifithrin α, a p53 transcriptional inhibitor [44]. Interestingly, an increase in cell proliferation was observed upon increasing the concentration of Pifithrin α (Fig. 4a–c). The cells treated with the different concentrations of curcumin along with the 10 μM Pifithrin α (24 h) showed reduced cytotoxicity (Fig. 4b). Increasing Pifithrin α concentration to 20 μM results in the complete abolishment of cytotoxic effects of curcumin ($P \leq 0.0001$) (Fig. 4b–c) [44]. Hence, it indicates that cell death is induced by CRp53-mediated apoptosis

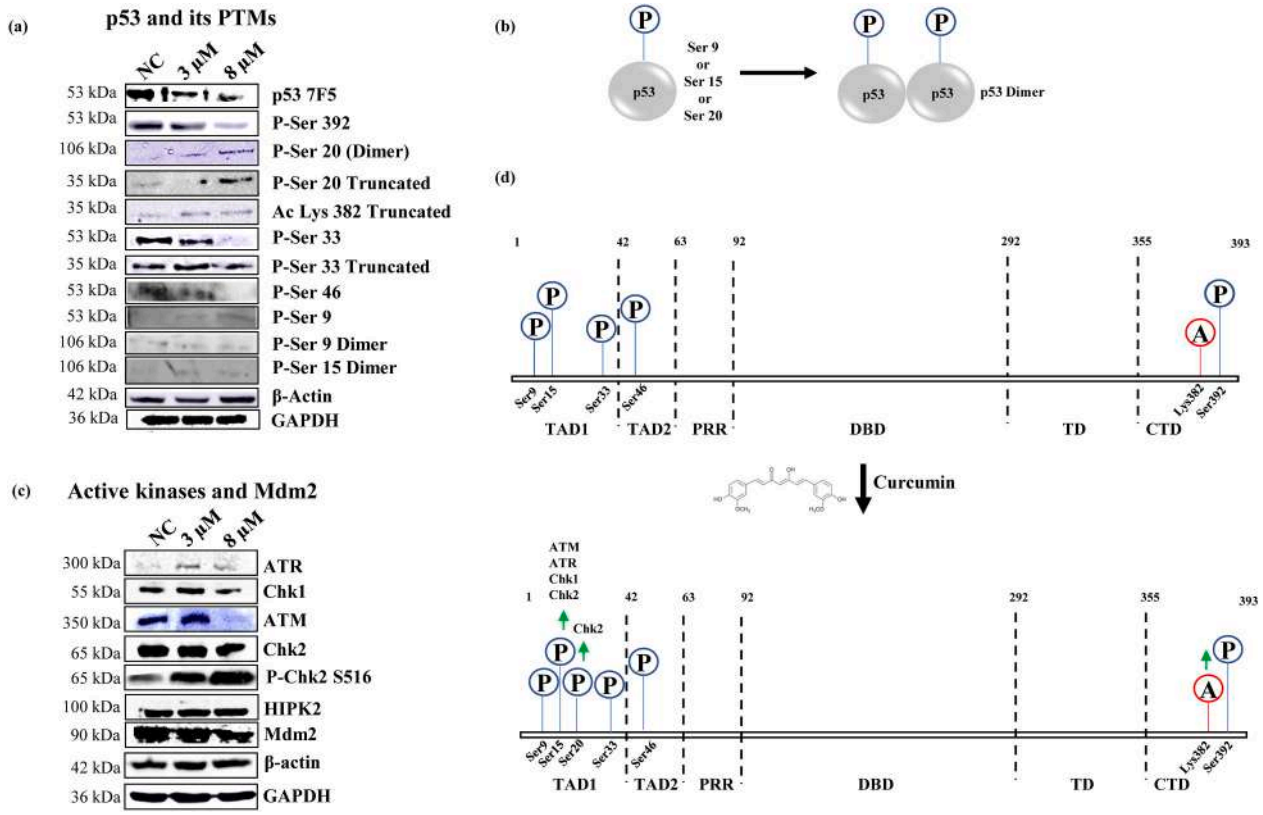

Fig. 3. Apoptosis and p53Y220C PTM analysis in BxPC-3 cells. (a) Western blot of p53Y220C with PTM-specific antibodies before and after 3 and 8 μM curcumin treatment. (b) Graphical representation of the various PTM responsible for the dimerization of the p53Y220C observed from the immunoblots analysis. (c) Western blot analysis of p53 phosphorylating kinase and Mdm2. (d) Graphical representation of PTMs in p53Y220C (native state) and after 8 μM curcumin treatment.

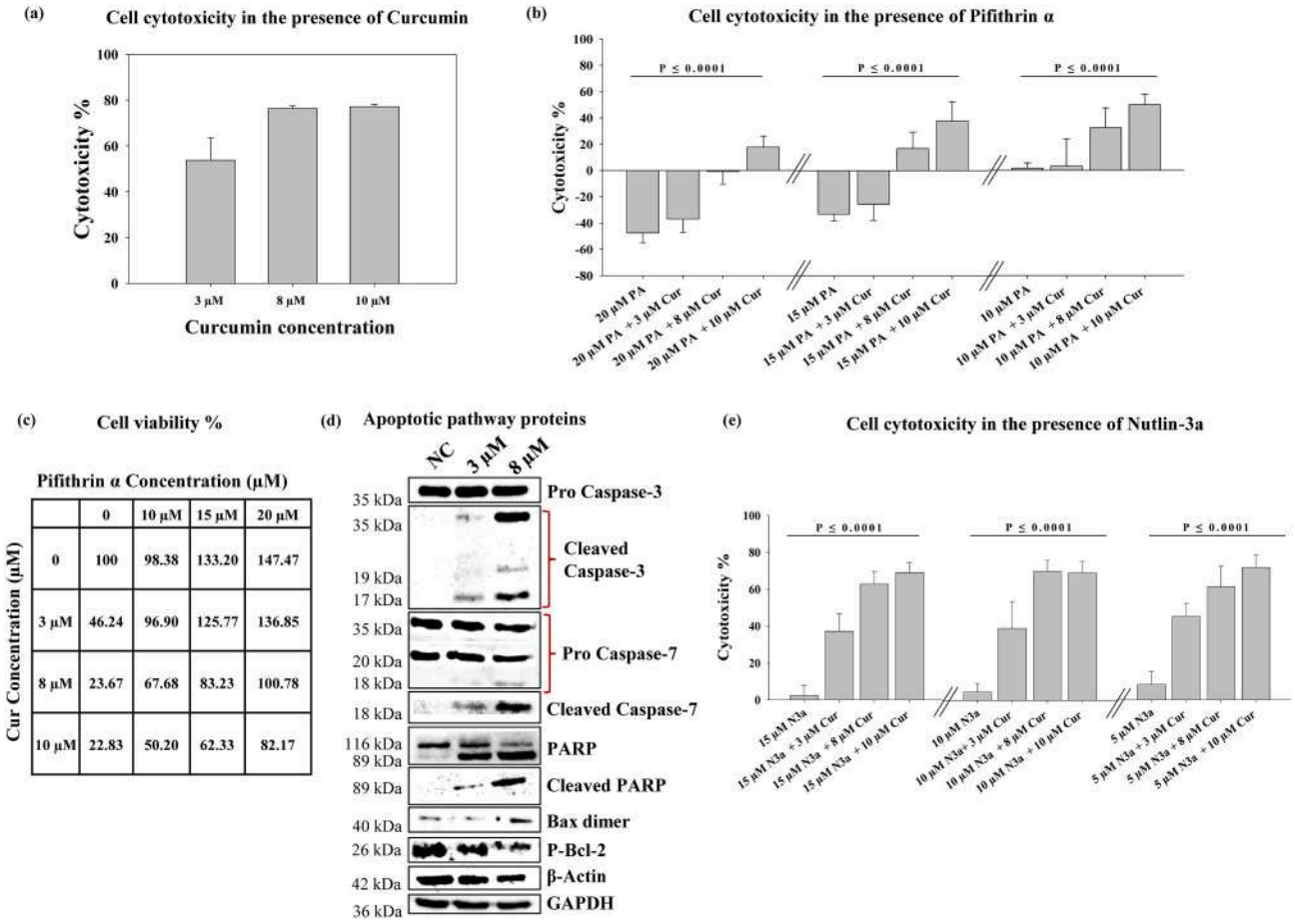

Fig. 4. Cytotoxicity in BxPC-3 cells in the presence and absence of curcumin, Pifithrin α and Nutlin-3a. (a) BxPC-3 cytotoxicity after 24 h of curcumin treatment. (b) MTT assay in the presence of 10, 15 and 20 μM Pifithrin α (PA) at different curcumin concentrations (3, 8 and 10 μM) (n = 8). (c) Cell viability in the presence and absence of different concentrations of curcumin and Pifithrin α. (d) Western blot of apoptotic markers Pro-caspase-3, Cleaved caspase-3, Pro caspase-7, Cleaved caspase-7, PARP, Cleaved PARP, Bax and P-Bcl-2 in the presence and absence of 3 and 8 μM curcumin indicating CRp53 mediated apoptosis. (e) MTT assay in the presence of 5, 10 and 15 μM Nutlin-3a (N3a) at different curcumin concentrations (3, 8 and 10 μM).

(Fig. 4a). Further, the expression of various apoptotic markers of the caspase-3 apoptotic pathway proteins was found to be significantly elevated compared to untreated cells (Figs. 4d, S4). Apart from that, activated cleaved caspase-7 and cleaved PARP levels were also found to be elevated with the increase in curcumin concentration (Figs. 4d, S4). The other evidence for the apoptosis mediated by CRp53 is the hyper-activation of Bax dimers and the downregulation of P-Bcl-2 protein (Figs. 4d, S4). The Bax hyperactivation is known to be mediated by p53 [68–70]. Thus, these findings confirmed that curcumin restores the transcription activity of the p53Y220C mutant.

3.8. CRp53 is resistant to Mdm2-mediated decay

To find that the CRp53 escapes Mdm2 mediated degradation, the BxPC-3 cells were treated with Nutlin-3a (Mdm2 inhibitor) [34,35] and different concentrations of curcumin (3, 8 and 10 μM) (Fig. 4e). No significant change or synergistic effect in cytotoxicity in the cells treated with both curcumin and Nutlin-3a compared to curcumin-treated cells (Fig. 4a and e). Even at a high concentration of Nutlin-3a (15 μM), the cytotoxicity was found to be similar to the 8 μM curcumin treatment. Thus, CRp53 escapes Mdm2 mediated proteasomal degradation and induces apoptosis in BxPC-3 cell lines.

3.9. Upregulation and downregulation of transcription targets by CRp53 in BxPC-3 cells

A significant change was observed in the whole-cell proteome of BxPC-3 cells before and after 8 μM curcumin treatment (24 h) (Figs. 5, S5a). The LFQ analysis showed a total of 227 dysregulated proteins with 159 found to be upregulated and 68 downregulated (Fig. 5a, Table S2). All the dysregulated proteins were categorized based on their cellular localization (Fig. 5b), gene ontologies, pathways, and protein class (Fig. S6a–c). Out of 227 genes, 180 are directly or indirectly regulated by p53 (Fig. S7). Based on the protein-protein interaction (PPI) analysis almost 180 proteins lie in the PPI network complex, containing 180 nodes and 869 edges as shown in Fig. S5b. Interestingly, by FI annotations using Cytoscape almost 140 dysregulated proteins are from 14 different cellular pathways (Figs. 5c, S5b, Table S3). In those, 31 proteins were found to be involved in apoptosis, cell cycle regulation, and the ER pathway (Fig. 5c). Based on the whole-cell LFQ data and other experiment results it indicates that CRp53 initiates apoptosis in BxPC-3 cell lines.

4. Discussion

In the past two decades, significant research is focused on the pharmacological development of small molecules to reactivate mutant p53 to prevent cancer progression. The mutation of residue Tyr at position 220 to Cys destabilizes p53 by ~4 kcal/mol making it non-

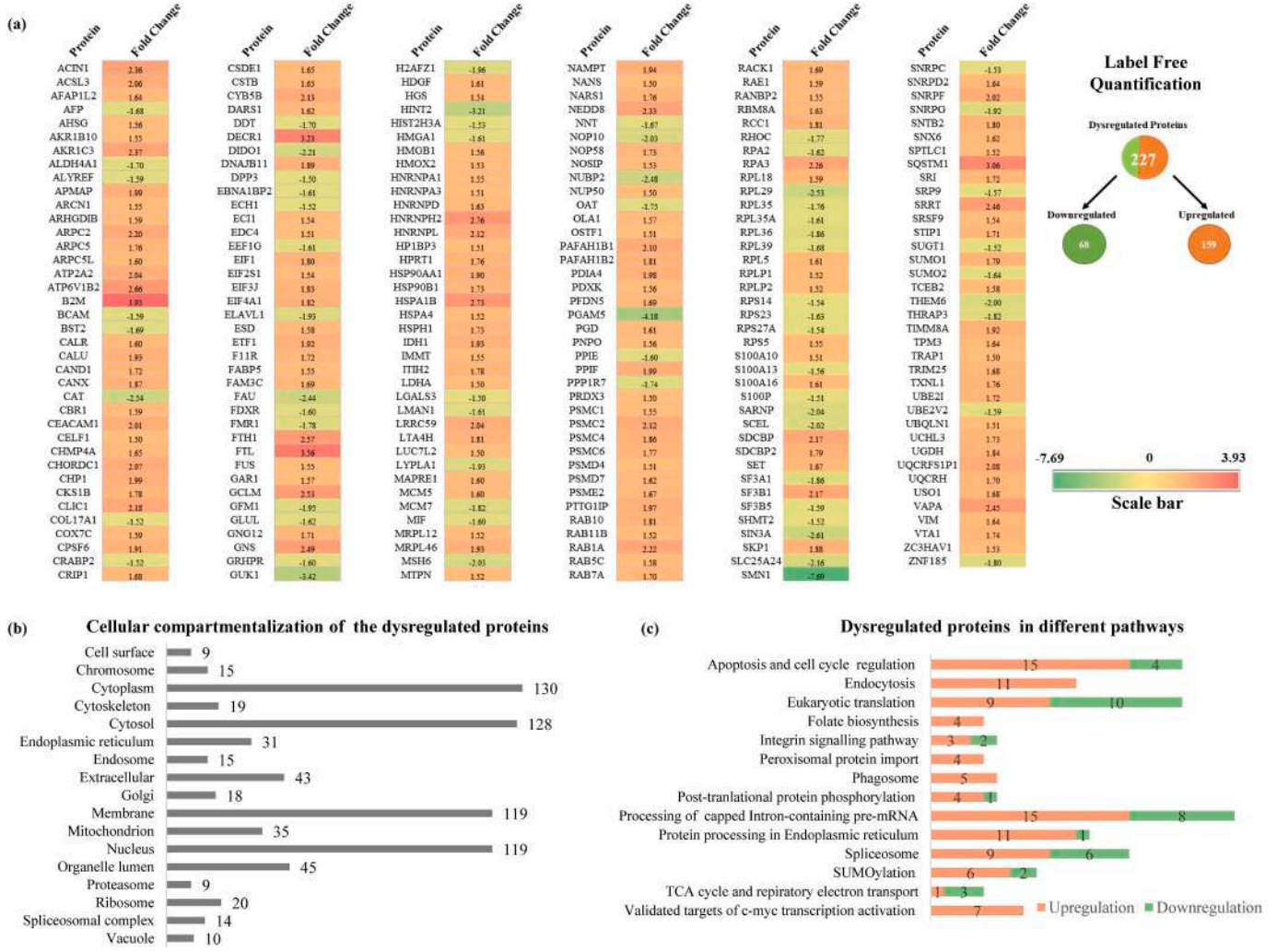

Fig. 5. Label-free quantification (LFQ) of the BxPC-3 cells before and after 8 μM curcumin treatment for 24 h. (a) The heat map shows the dysregulated proteins with ≥±1.5-fold change. The red color represents the upregulation, whereas the green color represents the downregulation. (b) Represents a graphical representation of the cellular compartmentalization of the dysregulated proteins. (c) Represents graphical distribution of dysregulated proteins in different pathways using Cystoscape software. (For interpretation of the references to color in this figure legend, the reader is referred to the web version of this article.)

functional in many cancers including pancreatic cancer leading to poor prognosis even after chemotherapy treatment [23]. But the mutant is also a promising target where its function can be restored with small molecule chaperones. In this study, we evaluated curcumin as a small molecule chaperone to restore mutant p53Y220C in pancreatic cancer cells. Like other reported small molecules [31–35,71], curcumin binds to the structural crevice between S3/S4 and S7/S8 loops and stabilizes the β-fold of mutant p53Y220C [36]. Curcumin binds with K_d of 17 μM compared to the other synthetic compounds (4 to 150 μM) reported so far and their binding affinities were measured for the p53 DNA binding domain whereas, here we report for the full-length mutant protein [31–35,38,71]. The synthetic compounds PK5196 and PK938 are reported to be the best cytotoxic compound with IC_{50} of 11 μM in BxPC-3 and 3.75 μM in HUH7 cell lines respectively with no reports on the active conformational state (PTM) of mutant p53. While in this study, we report curcumin with IC_{50} 3 to 8 μM with mutant p53 (CRp53) in a stable wild-type-like active conformation shown by our PTM and CD results. Our study also highlights that in the untreated BxPC-3 cell lines, the mutant p53Y220C forms pseudo-wild-type-like conformation with partial post-translational modifications (Fig. 3a and d). Upon curcumin treatment, an 8-fold increase in transcription activity of CRp53 was observed similar to other synthetic small molecule compounds reported so far [37,72] (Fig. 1d(i) and e (i)). The transcription activity is inhibited upon treating the cells with p53 transcription inhibitor Pifithrin α (Fig. 4b and c) confirming that the CRp53 is in functionally active state conformation mediating apoptosis in the BxPC-3 cell line. The increase in caspase-3 activity (Figs. 1e(iii), 4d) and upregulation of other pro-apoptotic markers Bax, Bcl-2 and PARP also support that the apoptotic pathways are initiated by CRp53 in BxPC-3 cell lines upon curcumin treatment [34,35,37]. Hence, based on our *in vivo*, *in vitro* and proteomics studies we propose a molecular mechanism for the activation of the apoptotic pathway by CRp53 in the BxPC-3 cell line (Fig. 6). Upon curcumin treatment, the mutant p53Y220C gets stabilized and activated by PI3 kinases like Chk1, ATM/ATR and HIPK kinases by post-translational modifications. The active CRp53 escapes the proteasomal degradation mediated by E3 ubiquitin ligase due to PTM and ribosomal protein 5 (RPL5) which prevents Mdm2 from binding to the active form of p53 [54,59,63,73]. The functionally active CRp53 further gets evenly distributed (especially migrated inside the nucleus) inside the cell to mediate apoptosis. In mitochondria, the active CRp53 gets translocated by peptidylprolyl cis/trans isomerase (PPIases) [55,60] (Fig. 6) and it regulates pro-apoptotic protein Bax to dimerize (Figs. 4d, S4) and form a pore in the mitochondrial outer membrane for the release of cytochrome C to initiate apoptosis [69,74–76]. The upregulation of cytochrome C oxidase subunit 7C (COX7C) [74] and the CSDE1 cold shock domain containing E1 in our LFQ data indicates the formation of apoptosomes

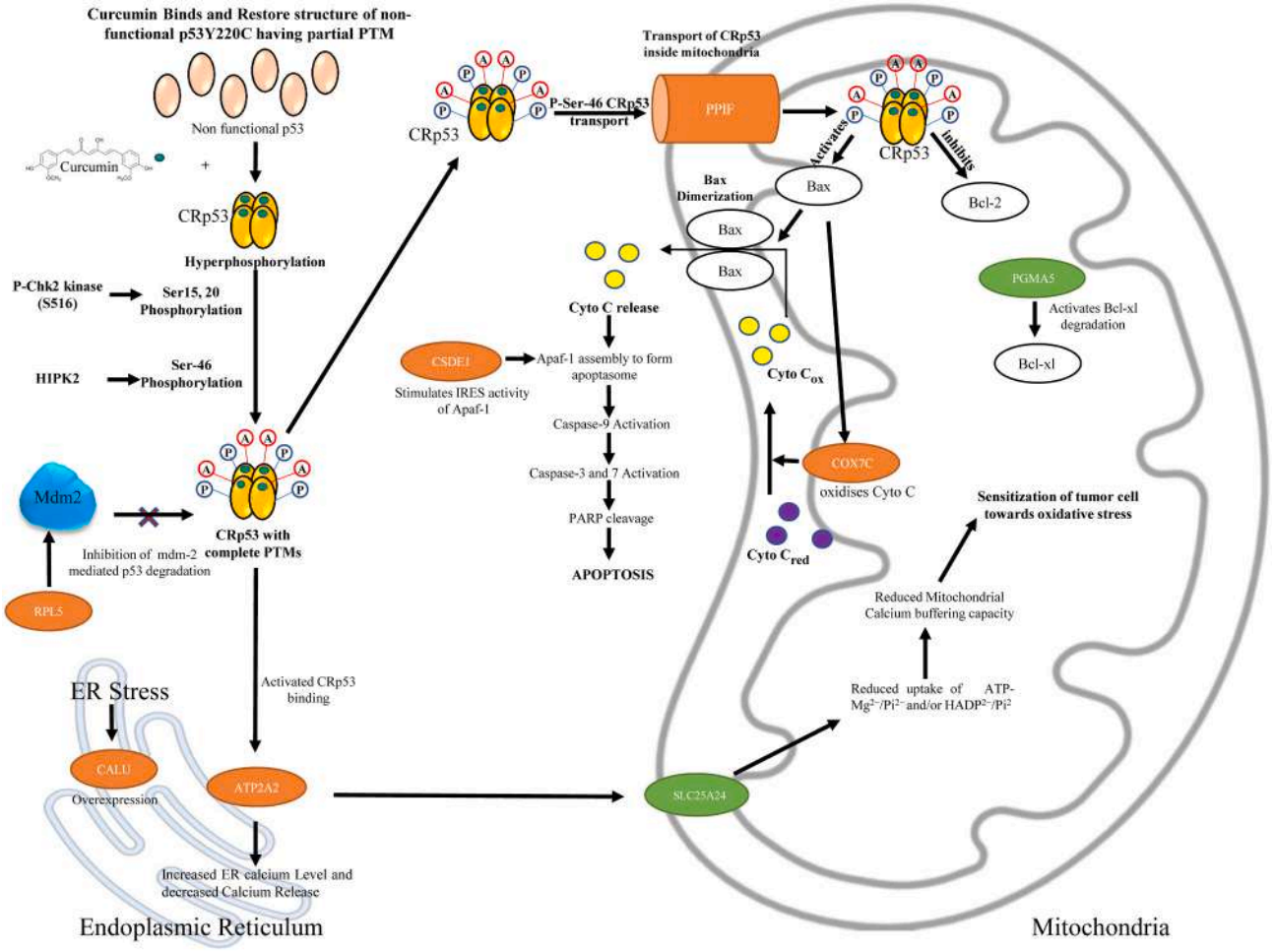

Fig. 6. The CRp53 mediated activation of transcription-dependent and independent apoptotic pathways based on the dysregulated proteins found in LFQ MS and immunoblot after 8 μM of curcumin treatment. (The orange color of protein represents hyperactivation and the green color of protein represents downregulation.) (For interpretation of the references to color in this figure legend, the reader is referred to the web version of this article.)

(Fig. 5a) [77]. Further, the apoptosome formation leads to the activation of caspase and PARP cleavage pathways of apoptosis (Fig. 4d). Similarly, in ER the CRp53 activates apoptotic signal through Ca^{2+} homeostasis by binding to calcium ATPase 2 (ATP2A2) in the sarcoplasmic/endoplasmic reticulum [78] which leads to calcium overload. As a result calcium deprivation happens in the cytosol, hence SLC25A24 gets downregulated resulting in decreased uptake of ATP/Mg^{2+} ions inside mitochondria causing a change in the morphology and activation of apoptosis [79] (Fig. 5a and 6). The upregulation of ATP2A2 and downregulation of calcium-binding mitochondrial carrier protein SLC25A24 in the LFQ data supports our proposed mechanism. Further, the dysregulation of other hallmark proteins like calumenin (CALU) and NAD(P) transhydrogenase, mitochondrial precursor (NNT) from the LFQ data also supports our proposed mechanism of activation of p53-mediated apoptosis inside ER and mitochondria (Fig. 5a, 6 and Table S4) [80,81]. Additionally, the LFQ data showed the activation of numerous genes from apoptotic programmed cell death pathways in BxPC-3 pancreatic cancer cell lines [82,83] (Tables S3 and S4).

Together all our data establish that curcumin rescues mutant p53Y220C and restores its wild-type-like function (Fig. 6). It is noteworthy that curcuminoids have been approved by the US Food and Drug Administration (FDA) as "Generally Recognized as Safe" (GRAS) and clinical trials have shown good tolerability to 12,000 mg/day of 95 % concentration of three curcuminoids: curcumin, bisdemethoxycurcumin, and demethoxycurcumin [84–86]. In summary, our study shows that targeting mutant p53Y220C with curcumin is an attractive combinatorial therapeutic option for future experimental and clinical studies in pancreatic cancer. Therefore, curcumin-based activation of mutant p53 can be one of the promising therapeutic strategies to control tumor progression.

Abbreviations

CRp53	Curcumin-rescued mutant p53Y220C
wt	Wild type
p53Y220C FL	p53Y220C full length
BLI	Bio-layer interferometry
CD	Circular dichroism
PTM	Post translational modification

Supplementary data to this article can be found online at https://doi.org/10.1016/j.bbamcr.2022.119343.

CRediT authorship contribution statement

L.M.: Methodology, Validation, Formal analysis, Investigation, Data curation, Graphics generation, Software, Writing, Review & editing, and Visualization. **S.S.:** Performed 2D gel electrophoresis experiment **H.G.:** Analysis of LFQ. **R.D.:** Analysis of cell-based assays. **V.M.:** Data curation. **R.S.S.:** Data curation. **P.K.:** Data curation. **A.S.E.:** Methodology, Validation, Formal analysis, Investigation, Data curation, Writing - Original draft, Writing - Review & editing and Visualization.

Uncited references

[43,48–50]

Declaration of competing interest

The authors have no substantial financial or commercial conflicts of interest with the current work or its publication.

Data availability

Data will be made available on request.

Acknowledgments

ASE thank All-India Institute of Medical Sciences, New Delhi for the Intramural grant A-678, LM thank DBT for the fellowship, SS thank the Indian Council of Medical Research for the research associate fellowship. We thank Dr. Rupesh K. Srivastava, Department of Biotechnology, AIIMS for the initial flow cytometry experiments.

Funding

This work was supported by Intramural grant A-678 of AIIMS (All India Institute of Medical Sciences), New Delhi as well as DBT project DRF:51 (Department of Biotechnology, India) contingency.

Ethical approval

The article does not involve any study with human participants or animals performed by any of the authors.

References

[1] M.B. Kastan, O. Onyekwere, D. Sidransky, B. Vogelstein, R.W. Craig, Participation of p53 protein in the cellular response to DNA damage, Cancer Res. 51 (1991) 6304–6311.
[2] N.J. Maclaine, T.R. Hupp, The regulation of p53 by phosphorylation: a model for how distinct signals integrate into the p53 pathway, Aging (Albany NY) 1 (2009) 490–502.
[3] K. Polyak, Y. Xia, J.L. Zweier, K.W. Kinzler, B. Vogelstein, A model for p53-induced apoptosis, Nature 389 (1997) 300–305, https://doi.org/10.1038/38525.
[4] S. Yogosawa, K. Yoshida, Tumor suppressive role for kinases phosphorylating p53 in DNA damage-induced apoptosis, Cancer Sci. 109 (2018) 3376–3382, https://doi.org/10.1111/cas.13792.
[5] B. Gu, W.-G. Zhu, Surf the post-translational modification network of p53 regulation, Int. J. Biol. Sci. 8 (2012) 672–684, https://doi.org/10.7150/ijbs.4283.
[6] M.J. Duffy, N.C. Synnott, S. O'Grady, J. Crown, Targeting p53 for the treatment of cancer, Semin. Cancer Biol. (2020), https://doi.org/10.1016/j.semcancer.2020.07.005.
[7] A. Parrales, T. Iwakuma, Targeting oncogenic mutant p53 for cancer therapy, Front. Oncol. 5 (2015) 288, https://doi.org/10.3389/fonc.2015.00288.
[8] F. Bunz, P.M. Hwang, C. Torrance, T. Waldman, Y. Zhang, L. Dillehay, J. Williams, C. Lengauer, K.W. Kinzler, B. Vogelstein, Disruption of p53 in human cancer cells alters the responses to therapeutic agents, J. Clin. Invest. 104 (1999) 263–269, https://doi.org/10.1172/JCI6863.
[9] E. Giovannetti, V. Mey, S. Nannizzi, G. Pasqualetti, M.D. Tacca, R. Danesi, Pharmacogenetics of anticancer drug sensitivity in pancreatic cancer, Mol. Cancer Ther. 5 (2006) 1387–1395, https://doi.org/10.1158/1535-7163.MCT-06-0004.
[10] X.-X. Sun, M.-S. Dai, H. Lu, 5-fluorouracil activation of p53 involves an MDM2-ribosomal protein interaction *, J. Biol. Chem. 282 (2007) 8052–8059, https://doi.org/10.1074/jbc.M610621200.
[11] J.P. Morton, P. Timpson, S.A. Karim, R.A. Ridgway, D. Athineos, B. Doyle, N. B. Jamieson, K.A. Oien, A.M. Lowy, V.G. Brunton, M.C. Frame, T.R.J. Evans, O. J. Sansom, Mutant p53 drives metastasis and overcomes growth arrest/senescence in pancreatic cancer, PNAS 107 (2010) 246–251, https://doi.org/10.1073/pnas.0908428107.
[12] S. Weissmueller, E. Manchado, M. Saborowski, J.P. Morris, E. Wagenblast, C. A. Davis, S.-H. Moon, N.T. Pfister, D.F. Tschaharganeh, T. Kitzing, D. Aust, E. K. Markert, J. Wu, S.M. Grimmond, C. Pilarsky, C. Prives, A.V. Biankin, S.W. Lowe, Mutant p53 drives pancreatic cancer metastasis through cell-autonomous PDGF receptor β signaling, Cell 157 (2014) 382–394, https://doi.org/10.1016/j.cell.2014.01.066.
[13] A. Peraud, F.W. Kreth, O.D. Wiestler, P. Kleihues, H.-J. Reulen, Prognostic impact of TP53 mutations and P53 protein overexpression in supratentorial WHO grade II astrocytomas and oligoastrocytomas, Clin. Cancer Res. 8 (2002) 1117–1124.
[14] S.A. Ahrendt, Y. Hu, M. Buta, M.P. McDermott, N. Benoit, S.C. Yang, L. Wu, D. Sidransky, p53 mutations and survival in stage I non-small-cell lung cancer: results of a prospective study, J. Natl. Cancer Inst. 95 (2003) 961–970, https://doi.org/10.1093/jnci/95.13.961.
[15] A.S. Coates, E.K. Millar, S.A. O'Toole, T.J. Molloy, G. Viale, A. Goldhirsch, M. M. Regan, R.D. Gelber, Z. Sun, M. Castiglione-Gertsch, B. Gusterson, E. A. Musgrove, R.L. Sutherland, Prognostic interaction between expression of p53 and estrogen receptor in patients with node-negative breast cancer: results from IBCSG trials VIII and IX, Breast Cancer Res. 14 (2012) R143, https://doi.org/10.1186/bcr3348.
[16] P. Yang, C.W. Du, M. Kwan, S.X. Liang, G.J. Zhang, The impact of p53 in predicting clinical outcome of breast cancer patients with visceral metastasis, Sci. Rep. 3 (2013) 2246, https://doi.org/10.1038/srep02246.
[17] S. Kato, S.-Y. Han, W. Liu, K. Otsuka, H. Shibata, R. Kanamaru, C. Ishioka, Understanding the function–structure and function–mutation relationships of p53 tumor suppressor protein by high-resolution missense mutation analysis, PNAS 100 (2003) 8424–8429, https://doi.org/10.1073/pnas.1431692100.
[18] X. Yue, Y. Zhao, Y. Xu, M. Zheng, Z. Feng, W. Hu, Mutant p53 in cancer: accumulation, gain-of-function, and therapy, J. Mol. Biol. 429 (2017) 1595–1606, https://doi.org/10.1016/j.jmb.2017.03.030.
[19] L. Malhotra, A. Singh, P. Kaur, A.S. Ethayathulla, Comprehensive omics studies of p53 mutants in human cancer, Brief. Funct. Genomics (2022), elac015, https://doi.org/10.1093/bfgp/elac015.
[20] K.H. Khoo, K.K. Hoe, C.S. Verma, D.P. Lane, Drugging the p53 pathway: understanding the route to clinical efficacy, Nat. Rev. Drug Discov. 13 (2014) 217–236, https://doi.org/10.1038/nrd4236.
[21] M. Mihara, S. Erster, A. Zaika, O. Petrenko, T. Chittenden, P. Pancoska, U.M. Moll, p53 has a direct apoptogenic role at the mitochondria, Mol. Cell 11 (2003) 577–590, https://doi.org/10.1016/s1097-2765(03)00050-9.
[22] S.G. Swisher, J.A. Roth, J. Nemunaitis, D.D. Lawrence, B.L. Kemp, C.H. Carrasco, D.G. Connors, A.K. El-Naggar, F. Fossella, B.S. Glisson, W.K. Hong, F.R. Khuri, J. M. Kurie, J.J. Lee, J.S. Lee, M. Mack, J.A. Merritt, D.M. Nguyen, J.C. Nesbitt, R. Perez-Soler, K.M. Pisters, J.B. Putnam, W.R. Richli, M. Savin, D.S. Schrump, D. M. Shin, A. Shulkin, G.L. Walsh, J. Wait, D. Weill, M.K. Waugh, Adenovirus-mediated p53 gene transfer in advanced non-small-cell lung cancer, J. Natl. Cancer Inst. 91 (1999) 763–771, https://doi.org/10.1093/jnci/91.9.763.
[23] A.N. Bullock, J. Henckel, A.R. Fersht, Quantitative analysis of residual folding and DNA binding in mutant p53 core domain: definition of mutant states for rescue in cancer therapy, Oncogene 19 (2000) 1245–1256, https://doi.org/10.1038/sj.onc.1203434.
[24] N. Issaeva, P. Bozko, M. Enge, M. Protopopova, L.G.G.C. Verhoef, M. Masucci, A. Pramanik, G. Selivanova, Small molecule RITA binds to p53, blocks p53-HDM-2 interaction and activates p53 function in tumors, Nat. Med. 10 (2004) 1321–1328, https://doi.org/10.1038/nm1146.
[25] J.M.R. Lambert, A. Moshfegh, P. Hainaut, K.G. Wiman, V.J.N. Bykov, Mutant p53 reactivation by PRIMA-1MET induces multiple signaling pathways converging on apoptosis, Oncogene 29 (2010) 1329–1338, https://doi.org/10.1038/onc.2009.425.
[26] L. Bouaoun, D. Sonkin, M. Ardin, M. Hollstein, G. Byrnes, J. Zavadil, M. Olivier, TP53 variations in human cancers: new lessons from the IARC TP53 database and genomics data, Hum. Mutat. 37 (2016) 865–876, https://doi.org/10.1002/humu.23035.
[27] W.A. Freed-Pastor, C. Prives, Mutant p53: one name, many proteins, Genes Dev. 26 (2012) 1268–1286, https://doi.org/10.1101/gad.190678.112.
[28] B. Leroy, J.L. Fournier, C. Ishioka, P. Monti, A. Inga, G. Fronza, T. Soussi, The TP53 website: an integrative resource centre for the TP53 mutation database and TP53 mutant analysis, Nucleic Acids Res. 41 (2013) D962–D969, https://doi.org/10.1093/nar/gks1033.
[29] R. Wilcken, G. Wang, F.M. Boeckler, A.R. Fersht, Kinetic mechanism of p53 oncogenic mutant aggregation and its inhibition, PNAS 109 (2012) 13584–13589, https://doi.org/10.1073/pnas.1211550109.
[30] G. Wang, A.R. Fersht, Propagation of aggregated p53: cross-reaction and coaggregation vs. seeding, Proc. Natl. Acad. Sci. U. S. A. 112 (2015) 2443–2448, https://doi.org/10.1073/pnas.1500262112.
[31] M.G.J. Baud, M.R. Bauer, L. Verduci, F.A. Dingler, K.J. Patel, D. Horil Roy, A. C. Joerger, A.R. Fersht, Aminobenzothiazole derivatives stabilize the thermolabile p53 cancer mutant Y220C and show anticancer activity in p53–Y220C cell lines, Eur. J. Med. Chem. 152 (2018) 101–114, https://doi.org/10.1016/j.ejmech.2018.04.035.
[32] M.R. Bauer, R.N. Jones, R.K. Tareque, B. Springett, F.A. Dingler, L. Verduci, K. J. Patel, A.R. Fersht, A.C. Joerger, J. Spencer, A structure-guided molecular chaperone approach for restoring the transcriptional activity of the p53 cancer mutant Y220C, FutureMed. Chem. 11 (2019) 2491–2504, https://doi.org/10.4155/fmc-2019-0181.
[33] F.M. Boeckler, A.C. Joerger, G. Jaggi, T.J. Rutherford, D.B. Veprintsev, A.R. Fersht, Targeted rescue of a destabilized mutant of p53 by an in silico screened drug, PNAS 105 (2008) 10360–10365, https://doi.org/10.1073/pnas.0805326105.
[34] P. Izetti, A. Hautefeuille, A.L. Abujamra, C.B. de Farias, J. Giacomazzi, B. Alemar, G. Lenz, R. Roesler, G. Schwartsmann, A.B. Osvaldt, P. Hainaut, P. Ashton-Prolla, PRIMA-1, a mutant p53 reactivator, induces apoptosis and enhances chemotherapeutic cytotoxicity in pancreatic cancer cell lines, Investig. New Drugs 32 (2014) 783–794, https://doi.org/10.1007/s10637-014-0090-9.
[35] X. Liu, R. Wilcken, A.C. Joerger, I.S. Chuckowree, J. Amin, J. Spencer, A.R. Fersht, Small molecule induced reactivation of mutant p53 in cancer cells, Nucleic Acids Res. 41 (2013) 6034–6044, https://doi.org/10.1093/nar/gkt305.

[36] L. Malhotra, H.K.V. Goyal, S. Jhuria, K. Dev, S. Kumar, M. Kumar, P. Kaur, A. S. Ethayathulla, Curcumin rescue p53Y220C in BxPC-3 pancreatic adenocarcinomas cell line: evidence-based on computational, biophysical, and in vivo studies, Biochim. Biophys. Acta Gen. Subj. 1865 (2021), 129807, https://doi.org/10.1016/j.bbagen.2020.129807.

[37] D. Sundar, Y. Yu, S.P. Katiyar, J.F. Putri, J.K. Dhanjal, J. Wang, A.N. Sari, E. Kolettas, S.C. Kaul, R. Wadhwa, Wild type p53 function in p53Y220C mutant harboring cells by treatment with Ashwagandha derived anticancer withanolides: bioinformatics and experimental evidence, J. Exp. Clin. Cancer Res. 38 (2019) 103, https://doi.org/10.1186/s13046-019-1099-x.

[38] M.R. Bauer, A.C. Joerger, A.R. Fersht, 2-Sulfonylpyrimidines: mild alkylating agents with anticancer activity toward p53-compromised cells, PNAS 113 (2016) E5271–E5280, https://doi.org/10.1073/pnas.1610421113.

[39] C. Luparello, I. Cruciata, A.C. Joerger, C.A. Ocasio, R. Jones, R.K. Tareque, M. C. Bagley, J. Spencer, M. Walker, C. Austin, T. Ferrara, P.D. Oca, R. Bellina, R. Branni, F. Caradonna, Genotoxicity and epigenotoxicity of carbazole-derived molecules on MCF-7 breast cancer cells, Int. J. Mol. Sci. 22 (2021) 3410, https://doi.org/10.3390/ijms22073410.

[40] E. Madan, T.M. Parker, M.R. Bauer, A. Dhiman, C.J. Pelham, M. Nagane, M. L. Kuppusamy, M. Holmes, T.R. Holmes, K. Shaik, K. Shee, S. Kiparoidze, S. D. Smith, Y.-S.A. Park, J.J. Gomm, L.J. Jones, A.R. Tomás, A.C. Cunha, K. Selvendiran, L.A. Hansen, A.R. Fersht, K. Hideg, R. Gogna, P. Kuppusamy, The curcumin analog HO-3867 selectively kills cancer cells by converting mutant p53 protein to transcriptionally active wildtype p53, J. Biol. Chem. 293 (2018) 4262–4276, https://doi.org/10.1074/jbc.RA117.000950.

[41] H. Müller-Esparza, M. Osorio-Valeriano, N. Steube, M. Thanbichler, L. Randau, Bio-layer interferometry analysis of the target binding activity of CRISPR-Cas effector complexes, Front. Mol. Biosci. 7 (2020) 98, https://doi.org/10.3389/fmolb.2020.00098.

[42] R.L. Petersen, Strategies using bio-layer interferometry biosensor technology for vaccine research and development, Biosensors (Basel) 7 (2017) E49, https://doi.org/10.3390/bios7040049.

[43] N.B. Shah, T.M. Duncan, Bio-layer interferometry for measuring kinetics of protein-protein interactions and allosteric ligand effects, J. Vis. Exp. (2014) 51383, https://doi.org/10.3791/51383.

[44] J. Zhu, M. Singh, G. Selivanova, S. Peuget, Pifithrin-α alters p53 post-translational modifications pattern and differentially inhibits p53 target genes, Sci. Rep. 10 (2020) 1049, https://doi.org/10.1038/s41598-020-58051-1.

[45] C. Jiang, H. Hu, B. Malewicz, Z. Wang, J. Lü, Selenite-induced p53 Ser-15 phosphorylation and caspase-mediated apoptosis in LNCaP human prostate cancer cells, Mol. Cancer Ther. 3 (2004) 877–884.

[46] Q. Zhang, W. Liu, H.-M. Zhang, G.-Y. Xie, Y.-R. Miao, M. Xia, A.-Y. Guo, hTFtarget: a comprehensive database for regulations of human transcription factors and their targets, Genomics Proteomics Bioinform. 18 (2020) 120–128, https://doi.org/10.1016/j.gpb.2019.09.006.

[47] Y. Perez-Riverol, A. Csordas, J. Bai, M. Bernal-Llinares, S. Hewapathirana, D. J. Kundu, A. Inuganti, J. Griss, G. Mayer, M. Eisenacher, E. Pérez, J. Uszkoreit, J. Pfeuffer, T. Sachsenberg, S. Yilmaz, S. Tiwary, J. Cox, E. Audain, M. Walzer, A. F. Jarnuczak, T. Ternent, A. Brazma, J.A. Vizcaíno, The PRIDE database and related tools and resources in 2019: improving support for quantification data, Nucleic Acids Res. 47 (2019) D442–D450, https://doi.org/10.1093/nar/gky1106.

[48] M. Kaneuchi, T. Yamashita, M. Shindoh, K. Segawa, S. Takahashi, I. Furuta, S. Fujimoto, K. Fujinaga, Induction of apoptosis by the p53–273L (Arg –> Leu) mutant in HSC3 cells without transactivation of p21Waf1/Cip1/Sdi1 and bax, Mol. Carcinog. 26 (1999) 44–52.

[49] J.M. Kokontis, A.J. Wagner, M. O'Leary, S. Liao, N. Hay, A transcriptional activation function of p53 is dispensable for and inhibitory of its apoptotic function, Oncogene 20 (2001) 659–668, https://doi.org/10.1038/sj.onc.1204139.

[50] K. Okaichi, L.H. Wang, J. Sasaki, H. Saya, M. Tada, Y. Okumura, A point mutation of human p53, which was not detected as a mutation by a yeast functional assay, led to apoptosis but not p21Waf1/Cip1/Sdi1 expression in response to ionizing radiation in a human osteosarcoma cell line, Saos-2, Int. J. Radiat. Oncol. Biol. Phys. 45 (1999) 975–980, https://doi.org/10.1016/s0360-3016(99)00285-0.

[51] A.L. Gartel, A.L. Tyner, The role of the cyclin-dependent kinase inhibitor p21 in apoptosis 1 supported in part by NIH Grant R01 DK56283 (to A. L. T.) for the p21 research and Campus Research Board and Illinois Department of Public Health Penny Severns Breast and Cervical Cancer grants (to A. L. G.).1, Mol. Cancer Ther. 1 (2002) 639–649.

[52] Y. Zhang, N. Fujita, T. Tsuruo, Caspase-mediated cleavage of p21 Waf1/Cip1 converts cancer cells from growth arrest to undergoing apoptosis, Oncogene 18 (1999) 1131–1138, https://doi.org/10.1038/sj.onc.1202426.

[53] S. Banin, L. Moyal, S. Shieh, Y. Taya, C.W. Anderson, L. Chessa, N.I. Smorodinsky, C. Prives, Y. Reiss, Y. Shiloh, Y. Ziv, Enhanced phosphorylation of p53 by ATM in response to DNA damage, Science 281 (1998) 1674–1677, https://doi.org/10.1126/science.281.5383.1674.

[54] J.R. Jabbur, P. Huang, W. Zhang, DNA damage-induced phosphorylation of p53 at serine 20 correlates with p21 and Mdm-2 induction in vivo, Oncogene 19 (2000) 6203–6208, https://doi.org/10.1038/sj.onc.1204017.

[55] R. Puca, L. Nardinocchi, D. Givol, G. D'Orazi, Regulation of p53 activity by HIPK2: molecular mechanisms and therapeutical implications in human cancer cells, Oncogene 29 (2010) 4378–4387, https://doi.org/10.1038/onc.2010.183.

[56] C.E. Canman, D.S. Lim, K.A. Cimprich, Y. Taya, K. Tamai, K. Sakaguchi, E. Appella, M.B. Kastan, J.D. Siliciano, Activation of the ATM kinase by ionizing radiation and phosphorylation of p53, Science 281 (1998) 1677–1679, https://doi.org/10.1126/science.281.5383.1677.

[57] D.W. Meek, C.W. Anderson, Posttranslational modification of p53: cooperative integrators of function, Cold Spring Harb. Perspect. Biol. 1 (2009), a000950, https://doi.org/10.1101/cshperspect.a000950.

[58] S. Saito, A.A. Goodarzi, Y. Higashimoto, Y. Noda, S.P. Lees-Miller, E. Appella, C. W. Anderson, ATM mediates phosphorylation at multiple p53 sites, including Ser (46), in response to ionizing radiation, J. Biol. Chem. 277 (2002) 12491–12494, https://doi.org/10.1074/jbc.C200093200.

[59] J. Loughery, M. Cox, L.M. Smith, D.W. Meek, Critical role for p53-serine 15 phosphorylation in stimulating transactivation at p53-responsive promoters, Nucleic Acids Res. 42 (2014) 7666–7680, https://doi.org/10.1093/nar/gku501.

[60] G. D'Orazi, B. Cecchinelli, T. Bruno, I. Manni, Y. Higashimoto, S. Saito, M. Gostissa, S. Coen, A. Marchetti, G. Del Sal, G. Piaggio, M. Fanciulli, E. Appella, S. Soddu, Homeodomain-interacting protein kinase-2 phosphorylates p53 at Ser 46 and mediates apoptosis, Nat. Cell Biol. 4 (2002) 11–19, https://doi.org/10.1038/ncb714.

[61] N.H. Chehab, A. Malikzay, E.S. Stavridi, T.D. Halazonetis, Phosphorylation of Ser-20 mediates stabilization of human p53 in response to DNA damage, PNAS 96 (1999) 13777–13782, https://doi.org/10.1073/pnas.96.24.13777.

[62] A. Nakamizo, T. Amano, W. Zhang, X.-Q. Zhang, L. Ramdas, T.-J. Liu, B.N. Bekele, T. Shono, T. Sasaki, W.F. Benedict, R. Sawaya, F.F. Lang, Phosphorylation of Thr18 and Ser20 of p53 in Ad-p53-induced apoptosis, Neuro-Oncology 10 (2008) 275–291, https://doi.org/10.1215/15228517-2008-015.

[63] T. Unger, T. Juven-Gershon, E. Moallem, M. Berger, R. Vogt Sionov, G. Lozano, M. Oren, Y. Haupt, Critical role for Ser20 of human p53 in the negative regulation of p53 by Mdm2, EMBO J. 18 (1999) 1805–1814, https://doi.org/10.1093/emboj/18.7.1805.

[64] X. Wu, J. Chen, Autophosphorylation of checkpoint kinase 2 at serine 516 is required for radiation-induced apoptosis, J. Biol. Chem. 278 (2003) 36163–36168, https://doi.org/10.1074/jbc.M303795200.

[65] T. Caspari, Checkpoints: how to activate p53, Curr. Biol. 10 (2000) R315–R317, https://doi.org/10.1016/S0960-9822(00)00439-5.

[66] A. Hirao, Y.Y. Kong, S. Matsuoka, A. Wakeham, J. Ruland, H. Yoshida, D. Liu, S. J. Elledge, T.W. Mak, DNA damage-induced activation of p53 by the checkpoint kinase Chk2, Science 287 (2000) 1824–1827, https://doi.org/10.1126/science.287.5459.1824.

[67] I. García-Santisteban, A. Llopis, L. Krenning, J. Vallejo-Rodríguez, B. van den Broek, A.M. Zubiaga, R.H. Medema, Sustained CHK2 activity, but not ATM activity, is critical to maintain a G1 arrest after DNA damage in untransformed cells, BMC Biol. 19 (2021) 35, https://doi.org/10.1186/s12915-021-00965-x.

[68] J.E. Chipuk, T. Kuwana, L. Bouchier-Hayes, N.M. Droin, D.D. Newmeyer, M. Schuler, D.R. Green, Direct activation of Bax by p53 mediates mitochondrial membrane permeabilization and apoptosis, Science 303 (2004) 1010–1014, https://doi.org/10.1126/science.1092734.

[69] T. Miyashita, S. Krajewski, M. Krajewska, H.G. Wang, H.K. Lin, D.A. Liebermann, B. Hoffman, J.C. Reed, Tumor suppressor p53 is a regulator of bcl-2 and bax gene expression in vitro and in vivo, Oncogene 9 (1994) 1799–1805.

[70] A.V. Vaseva, U.M. Moll, The mitochondrial p53 pathway, Biochim. Biophys. Acta Bioenerg. 1787 (2009) 414–420, https://doi.org/10.1016/j.bbabio.2008.10.005.

[71] R. Wilcken, X. Liu, M.O. Zimmermann, T.J. Rutherford, A.R. Fersht, A.C. Joerger, F.M. Boeckler, Halogen-enriched fragment libraries as leads for drug rescue of mutant p53, J. Am. Chem. Soc. 134 (2012) 6810–6818, https://doi.org/10.1021/ja301056a.

[72] N. Radhakrishnan, J.K. Dhanjal, A.N. Sari, Y. Ishida, K. Terao, S.C. Kaul, D. Sundar, R. Wadhwa, Caffeic acid phenethyl ester (CAPE) confers wild type p53 function in p53Y220C mutant: bioinformatics and experimental evidence, Discov. Oncol. 12 (2021) 64, https://doi.org/10.1007/s12672-021-00461-2.

[73] Y. Zhao, S. Lu, L. Wu, G. Chai, H. Wang, Y. Chen, J. Sun, Y. Yu, W. Zhou, Q. Zheng, M. Wu, G.A. Otterson, W.-G. Zhu, Acetylation of p53 at lysine 373/382 by the histone deacetylase inhibitor depsipeptide induces expression of p21(Waf1/Cip1), Mol. Cell. Biol. 26 (2006) 2782–2790, https://doi.org/10.1128/MCB.26.7.2782-2790.2006.

[74] G.C. Brown, V. Borutaite, Regulation of apoptosis by the redox state of cytochrome c, Biochim. Biophys. Acta Bioenerg. 1777 (2008) 877–881, https://doi.org/10.1016/j.bbabio.2008.03.024.

[75] M. Schuler, E. Bossy-Wetzel, J.C. Goldstein, P. Fitzgerald, D.R. Green, p53 induces apoptosis by caspase activation through mitochondrial cytochrome c release *, J. Biol. Chem. 275 (2000) 7337–7342, https://doi.org/10.1074/jbc.275.10.7337.

[76] M. Zhang, J. Zheng, R. Nussinov, B. Ma, Release of cytochrome C from Bax pores at the mitochondrial membrane, Sci. Rep. 7 (2017) 2635, https://doi.org/10.1038/s41598-017-02825-7.

[77] A.-X. Guo, J.-J. Cui, L.-Y. Wang, J.-Y. Yin, The role of CSDE1 in translational reprogramming and human diseases, Cell Commun. Signal. 18 (2020) 14, https://doi.org/10.1186/s12964-019-0496-2.

[78] C. Giorgi, M. Bonora, G. Sorrentino, S. Missiroli, F. Poletti, J.M. Suski, F. G. Ramirez, R. Rizzuto, F.D. Virgilio, E. Zito, P.P. Pandolfi, M.R. Wieckowski, F. Mammano, G.D. Sal, P. Pinton, p53 at the endoplasmic reticulum regulates apoptosis in a Ca2+-dependent manner, PNAS 112 (2015) 1779–1784, https://doi.org/10.1073/pnas.1410723112.

[79] J. Traba, A. del Arco, M.R. Duchen, G. Szabadkai, J. Satrústegui, SCaMC-1 promotes cancer cell survival by desensitizing mitochondrial permeability transition via ATP/ADP-mediated matrix Ca2+ buffering, Cell Death Differ. 19 (2012) 650–660, https://doi.org/10.1038/cdd.2011.139.

[80] H.-Y. Ho, Y.-T. Lin, G. Lin, P.-R. Wu, M.-L. Cheng, Nicotinamide nucleotide transhydrogenase (NNT) deficiency dysregulates mitochondrial retrograde signaling and impedes proliferation, Redox Biol. 12 (2017) 916–928, https://doi.org/10.1016/j.redox.2017.04.035.

[81] J.H. Lee, E.J. Kwon, D.H. Kim, Calumenin has a role in the alleviation of ER stress in neonatal rat cardiomyocytes, Biochem. Biophys. Res. Commun. 439 (2013) 327–332, https://doi.org/10.1016/j.bbrc.2013.08.087.
[82] R. Osman, P. Tacnet-Delorme, J.-P. Kleman, A. Millet, P. Frachet, Calreticulin release at an early stage of death modulates the clearance by macrophages of apoptotic cells, Front. Immunol. 8 (2017), https://doi.org/10.3389/fimmu.2017.01034.
[83] J.M. Tarr, P.J. Young, R. Morse, D.J. Shaw, R. Haigh, P.G. Petrov, S.J. Johnson, P. G. Winyard, P. Eggleton, A mechanism of release of calreticulin from cells during apoptosis, J. Mol. Biol. 401 (2010) 799–812, https://doi.org/10.1016/j.jmb.2010.06.064.
[84] P. Basnet, N. Skalko-Basnet, Curcumin: an anti-inflammatory molecule from a curry spice on the path to cancer treatment, Molecules 16 (2011) 4567–4598, https://doi.org/10.3390/molecules16064567.
[85] S.C. Gupta, S. Patchva, B.B. Aggarwal, Therapeutic roles of curcumin: lessons learned from clinical trials, AAPS J. 15 (2012) 195–218, https://doi.org/10.1208/s12248-012-9432-8.
[86] C.D. Lao, M.T. Ruffin, D. Normolle, D.D. Heath, S.I. Murray, J.M. Bailey, M. E. Boggs, J. Crowell, C.L. Rock, D.E. Brenner, Dose escalation of a curcuminoid formulation, BMC Complement. Altern. Med. 6 (2006) 10, https://doi.org/10.1186/1472-6882-6-10.